Z. Phys. Chem. **226** (2012) 177–183 / **DOI** 10.1524/zpch.2012.0147

Synthesis of $LiFePO_4$ by Ultrasonic and Nozzle Spray Pyrolysis

By Manuela Jüstel[1,*], Albrecht Schwinger[2], Bernd Friedrich[2], and Michael Binnewies[1]

[1] Institute of Inorganic Chemistry, Leibniz University of Hannover, Callinstraße 9, 30167 Hannover, Germany
[2] Department of Metallurgical Process Technology and Metal recycling, RWTH Aachen, Intzestraße 3, 52056 Aachen, Germany

(Received July 6, 2011; accepted in revised form September 23, 2011)

Lithium Iron Phosphate / Spray Pyrolysis / Particle Formation

Lithium iron phosphate $LiFePO_4$ (LFP) is one of the promising new cathode materials for next generation lithium secondary batteries. Various synthesis strategies have been proposed to create $LiFePO_4$ particles with maximum efficiency. The spray pyrolysis is a suitable synthesis technique which allows to direct the particle formation in multiple ways. $LiFePO_4$ has successfully been synthesized by ultrasonic and nozzle spray pyrolysis. The obtained products were characterized by means of XRD and SEM analysis. Furthermore, the mechanism of the particle formation was investigated.

1. Introduction

New, low cost cathode material with high performance as well as high safety standards have been the aim of copious investigations of various researcher groups around the world. Among the most promising substances are lithium metal phosphates. Especially the olivine structured triphylite $LiFePO_4$, which was first proposed by Padhi *et al.* in 1997, seems promising. Its redox potential *vs.* Li/Li^+ is 3.4 V whereas the theoretical capacity is 170 mA h/g [1,2].

One reason for its great potential is that iron, the redox active species in this material, has a comparatively high Clarke number of 4.7% [3]. The Clarke number is an estimation of the abundance of an element in the outermost shell of the earth. Due to its high value iron is considered to be among the five most common elements in the earth crust. In consequence, $LiFePO_4$ is a potentially low cost active material. Furthermore, it is nontoxic, environmentally benign and less prone to oxygen loss than other oxide based cathode materials thus ensuring high safety [4,5]. Yet $LiFePO_4$ has a major disadvantage: Its intrinsic electronic conductivity is only 10^{-9} S/cm [6].

* Corresponding author. E-mail: juestel@aca.uni-hannover.de

In order to create a usable cathode material, the conductivity has to be enhanced by several orders of magnitudes. The reduction of the particle size, doping with aliovalent ions and the coating with an conductive agent are among the most popular approaches to achieve this [4,7,8].

The spray pyrolysis is a suitable synthesis technique which allows to direct the product formation in several ways. All three strategies to optimize the performance of $LiFePO_4$ can be realized and combined by this method [9].

In this paper, we focus on the comparison of the synthesis of pure $LiFePO_4$ particles via the ultrasonic and nozzle spray pyrolysis. By using adequate additives, coated as well as doped $LiFePO_4$ samples have been prepared by both of these methods as well. However, a detailed discussion of these would go beyond the aim of this paper.

2. Experimental

2.1 Spray pyrolysis

The term spray pyrolysis refers to synthesis methods in which a precursor solution is atomized into a fine aerosol and afterwards conducted to a hot furnace where the particle formation takes place.

A major advantage of this process is that the initial precursor solution has a homogenous ingredient distribution down to the atomic level [10]. This makes it an ideal method for the preparation of doped materials with a uniform ion arrangement. Furthermore particle size, size distribution and morphology can be effectively controlled and thus defined, not agglomeration particles with a spherical geometry synthesized [11].

The formation of the aerosol can be achieved by two different methods. Ultrasonic spray pyrolysis utilizes an ultrasonic generator to transfer vibration energy to a liquid. At sufficient frequencies a fine spray with defined droplet size forms at the crests of the generated waves [12].

The nozzle spray pyrolysis achieves the aerosol formation through the use of a pneumatic or two-fluid nozzle. The work principal of this nozzle type is based on the mechanic forces that occur when a gas with a high speed strikes a motionless liquid. The surface tension of the liquid is overcome by the high frictional sharing forces and a fine spray is created [13].

2.2 Ultrasonic spray pyrolysis

A homogenous 0.05 M precursor solution was prepared by dissolving stoichiometric amounts of $FeCl_2$ (98%, Alfa Aesar), LiCl (> 99%, Merck) and H_3PO_4 (85%, Merck) in distilled water. Afterwards, the solution was filled in an ultrasonic nebulizer (RBI). The atomization was carried out with an operating frequency of 2.5 MHz. An inert nitrogen flow transported the droplets from the ultrasonic generator through a quartz tube into the reaction furnace which was kept at 800 °C . The length of the heating zone is 40 cm, resulting in an average residence time of 2.4 s. The particles, which were formed in the furnace, were collected with the aid of three gas wash bottles that have previously been filled with distilled water. After the reaction the final product was separated by sedimentation and dried at 80 °C in a drying cabinet.

A schematic diagram of the experimental setup can be seen in Fig. 1.

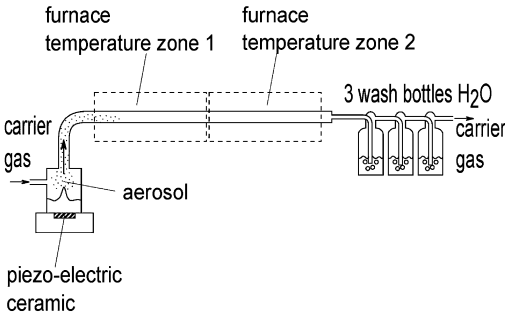

Fig. 1. Experimental setup of the ultrasonic spray pyrolysis.

2.3 Nozzle spray pyrolysis

Prior to synthesis the whole reactor was flushed with an inert argon flow to ensure the absence of oxygen during the particle formation. A 0.1 M homogenous precursor solution was prepared by dissolving stoichiometric amounts of $FeCl_2 \cdot 4H_2O$ (99%, Acros), LiCl (99%, Aldrich) and H_3PO_4 (85%, Budenheim) in distilled water. The solution was placed in the reservoir of a two-fluid nozzle which utilized nitrogen with an initial pressure of 1 bar as atomization gas. The hereby generated fine aerosol was transferred to the reaction chamber. This chamber consisted of a quartz tube with a diameter of 2.9 cm within a hot wall furnace that was kept at 800 °C . The length of the heating zone was 58 cm, thus, an average residence time of 1 s was achieved. After the particle formation, the final product was collected through sedimentation processes in a round bottom flask.

A schematic diagram of the experimental setup can be seen in Fig. 2.

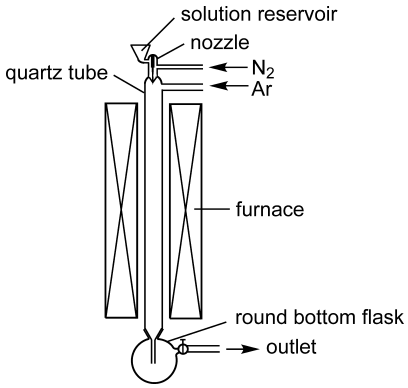

Fig. 2. Experimental setup of the nozzle spray pyrolysis.

3. Mechanism of particle formation

The mechanism of the particle formation is the same regardless how the initial droplets have been produced.

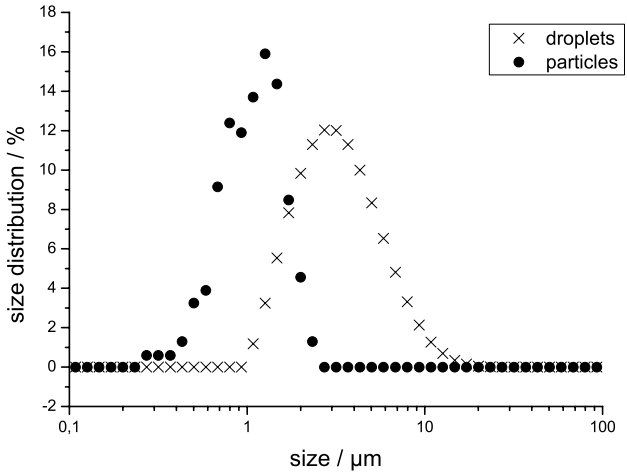

Fig. 3. Droplet and particle size distribution of the ultrasonic spray pyrolysis.

The particle formation takes place in the reaction furnaces. Due to the high temperatures the droplets heat up and solvent evaporation starts. This phenomenon does not occur in the whole droplet at the same time but rather sets in at the droplet rim first. Water molecules start to evaporate from the droplet surface and are lost to the surrounding gas phase. Thus a shrinking of the droplet is initialized. Through the water evaporation at the droplet rim an increase of the precursor concentration in this area is triggered. In turn, this causes a diffusion of precursor molecules towards the droplet center [14,15].

As soon as the critical supersaturation is reached, a homogenous nucleation sets in via precipitation processes. Due to the higher precursor concentrations at the droplet rim, this is first the case at the outer spheres of the droplet. After primary nuclei have been formed, heterogonous nuclei growth starts and spreads to regions with lower ingredients concentrations. Figure 3 displays the relation between the initial droplet size and the dimensions of the obtained particles synthesized by ultrasonic spray pyrolysis. The results for the nozzle spray pyrolysis are analog. The droplet size was determined by a Sympatec-Helos laser particle size spectrometer. The process parameters during the measurement were the same as in the actual particle formation experiments. The particle size distribution was obtained by analyzing the dimensions of two hundred and fifty randomly selected particles on SEM images using the programs ImageJ, Microsoft Photoshop and OriginPro8.

As can been seen, the particle size is in average slightly smaller than the droplet size. The reason for this is that the particle formation only sets in as soon as the critical supersaturation is reached. This in turn is not the case until the droplet starts to shrink, due to the loss of water molecules.

Depending on the droplet size, the precursor concentration and the evaporation rate hollow or entirely solid particles can form. Whereas big droplets, low precursor concentrations and fast evaporation rates favor the formation of hollow particles, the synthesis is directed towards volumetrically solid particles by small droplets, high precursor concentrations and slow evaporation rates [14,15].

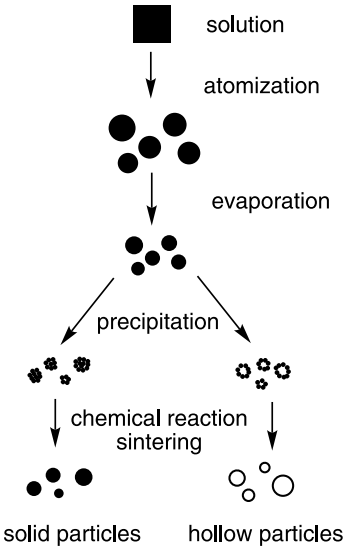

Fig. 4. Mechanism of the particle formation.

A schematic overview of the particle formation is provided in Fig. 4.

In order to determine if $LiFePO_4$ is already formed at the initial precipitation step or if intermediate products occur, which react in a subsequent solid state like reaction towards the desired product, further experiments were carried out. For this purpose, small quantities of the starting solutions were evaporated under an inert atmosphere at 80 respectively 150 °C. X-ray diffraction measurements with a Stoe Stadi P diffractometer using Cu K_α radiation revealed $FeCl_2 \cdot 4H_2O$ to be a component of the precipitation process. Further compounds have not been detected yet.

It is therefore assumed that the initial chlorides precipitate first. Only afterwards, the final product $LiFePO_4$ is formed in a solid state like synthesis.

4. Results

X-ray diffraction patterns of the products obtained by ultrasonic and nozzle spray pyrolysis were collected using a Stoe Stadi P diffractometer utilizing Cu K_α radiation and analyzed with the program $WinX^{Pow}$. The patterns are in good agreement with one an another and could be assigned to the ICDD reference number [40-1499] which belongs to $LiFePO_4$. No differences regarding purity or crystallinity were found within the patterns obtained by ultrasonic respectively nozzle spray pyrolysis.

Crystalline $LiFePO_4$ has therefore successfully been synthesized via the ultrasonic and nozzle spray pyrolysis technique. The recorded XRD patterns are shown in Fig. 5.

The particle morphology was investigated by scanning electron microscope images using a FEI-Philips XL 30. With both synthesis methods, spherical, non agglomerated particles were obtained, as can be seen in Fig. 6. The particles' surfaces show multiple

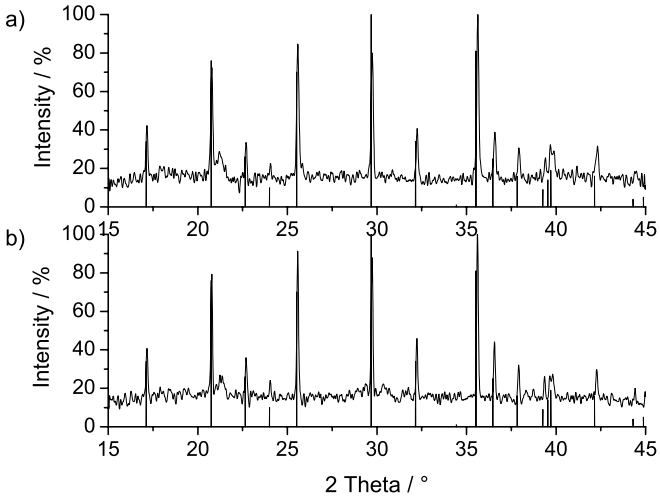

Fig. 5. XRD patter product maintained by ultrasonic spray pyrolysis a); XRD pattern of the product obtained by nozzle spray pyrolysis b).

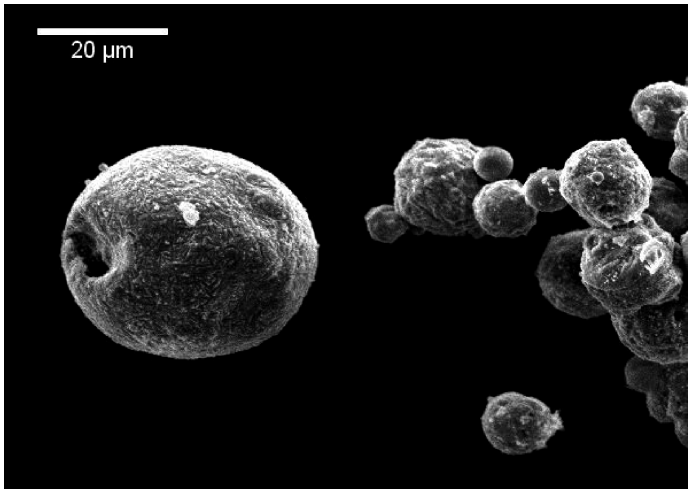

Fig. 6. SEM image of the particles maintained by nozzle spray pyrolysis.

textures. This confirms that the nucleation sets in simultaneously at various places of the droplet rim. At first each nucleation side starts to grow individually with a distinct surface finish. Only after spreading into the growth zone of another nucleus, the two phases are annealed, thus forming the rich surface texture of the resulting particle.

Furthermore, our investigations showed that the particle sizes of the obtained products are slightly smaller than the initial droplet sizes. This indicates that nucleation must set in shortly after water evaporation starts.

5. Conclusion

Crystalline $LiFePO_4$ was successfully synthesized via the ultrasonic and nozzle spray pyrolysis. The mechanism of the particle formation was found to be independent of the method used for the atomization of the precursor solution. No essential difference could be detected between the powders synthesized by ultrasonic respectively nozzle spray pyrolysis.

Furthermore, we were able to identify $FeCl_2 \cdot 4H_2O$ as an intermediate product of the formation reaction of $LiFePO_4$. The particles of the obtained products were found to be of slightly smaller dimension than the original droplets. This result indicates that critical supersaturation is reached shortly after the shrinking of the droplet is initialized. Reaching the critical supersaturaion triggers nucleation processes and leads to the final product in form of spherical, non agglomerated primary particles without any detectable sintering necks.

This particle morphology makes the spray pyrolysis a suitable synthesis technique for $LiFePO_4$. Due to the fact that other synthesis techniques often require high process temperatures and long residence time, individually existing, non agglomerated and not sintered $LiFePO_4$ particles are difficult to obtain. This applies, for example, for the solid state synthesis or the sol gel process [4,16].

Through further research on the spray pyrolytic preparation of $LiFePO_4$ particles with aliovalent ion doping respectively carbon coating, the authors anticipate to succeed in synthesizing a capable cathode material for lithium ion batteries.

Acknowledgement

The authors wish to thank the German Federal Ministry of Education and Research (BMBF) for the financial support in the course of the LiVe-Project.

References

1. M. S. Whittingham, Chem. Rev. **104** (2004) 4271.
2. G. Cheruvally, *Lithium Iron Phosphate: A Promising Cathothe-Active Material for Lithium Secondary Batteries*. Trans Tech Publications, Zurich (2008).
3. F. W. Clarke and H. S. Washington, U. S. Geol. Survey **127** (1924) 112.
4. D. Jugović and D. Uskoković, J. Power Sources **190** (2009) 538.
5. S. Nishimura *et al.*, Nat. Mater. **7** (2008) 707.
6. K. Ozawa (Ed.), *Lithium Ion Rechargeable Batteries*. Wiley-VCH Verlag GmbH & Co: Weinheim (2009).
7. S.-Y. Chung, J. T. Bloking, and Y.-M. Chiang, Nat. Mater. **1** (2002) 123.
8. J. D. Wilcox *et al.*, J. Elechtrochem. Soc. **154** (2007) A389.
9. M. Konarova and I. Taniguchi, J. Power Sources **195** (2010) 3661.
10. S. L. Bewlay *et al.*, Mater. Lett. **58** (2004) 1788.
11. L. S. Gomez et.al., Electrochim. Acta **55** (2010) 2805.
12. S. Stopić *et al.*, Metalurgija **14** (2008) 41.
13. P. D. Hede, P. Bach, and A. D. Jensen, Chem. Eng. Sci. **63** (2008) 3821.
14. G. V. Jayanthi, S. C. Zhang, and G. L. Messing, Aerosol Sci. Technol. **19** (1993) 478.
15. M. Eslamian, M. Ahmed, and N. Ashgriz, Nanotechnology **17** (2006) 1674.
16. S. Scaccia *et al.*, Mater. Res. Bull. **38** (2005) 1155.